Lower Miocene gypsum palaeokarst in the Madrid Basin (central Spain): dissolution diagenesis, morphological relics and karst end-products

JUAN P. RODRÍGUEZ-ARANDA, JOSÉ P. CALVO and M. ESTHER SANZ-MONTERO
Departamento de Petrología y Geoquímica, Facultad de CC Geológicas Universidad Complutense, 28040 Madrid, Spain (E-mail: jpcalvo@geo.ucm.es)

ABSTRACT

The Miocene sedimentary record of the Madrid Basin displays several examples of palaeokarstic surfaces sculpted within evaporite formations. One of these palaeokarstic surfaces represents the boundary between two main lithostratigraphic units, the Miocene Lower and Intermediate units of the Madrid Basin. The palaeokarst formed in lacustrine gypsum deposits of Aragonian age and corresponds to a surface palaeokarst (epikarst), further buried by terrigenous deposits of the overlying unit. Karst features are recognized up to 5.5 m beneath the gypsum surface. Exokarst and endokarst zones are distinguished by the spatial distribution of solution features, i.e. karren, dolines, pits, conduits and caves, and collapse breccias, sedimentary fills and alteration of the original gypsum across the karst profiles. The development of the gypsum palaeokarst began after drying out of a saline lake basin, as supported by recognition of root tubes, later converted to cylindrical and funnel-shaped pits, at the top of the karstic profiles. The existence of a shallow water table along with low hydraulic gradients was the main factor controlling the karst evolution, and explains the limited depth reached by both exokarst and endokarst features. Synsedimentary fill of the karst system by roughly laminated to massive clay mudstone with subordinate carbonate and clastic gypsum reflects a punctuated sedimentation regime probably related to episodic heavy rainfalls typical of arid to semi-arid climates. Duration of karstification is of the order of several thousands of years, which is consistent with previous statements that gypsum karstification can develop rapidly over geologically short time periods.

Keywords Gypsum deposits, karstification processes, Madrid Basin, Miocene, palaeokarst.

INTRODUCTION

Palaeokarst refers to karstic (solution-related) features formed in the past, related to an earlier hydrological system or land surface (Wright, 1991). According to this definition, a palaeokarst records basically those morphological and geological features that can be expected from a modern karst system. Yet in a palaeokarst, the hydrological function has been lost and, consequently, it is not adjusted to the present dynamic controlling factor (Jennings, 1985; Klimchouk, 1996a).

Most studies of karst systems are concerned with soluble carbonate rocks (Jennings, 1971; Bögli, 1980; Esteban & Klappa, 1983; Ford, 1988; Ford & Williams, 1989; Smart & Whitaker, 1991), whereas highly soluble evaporite formations showing karstification are considerably less documented (Warren *et al.*, 1990; Gutiérrez, 1996; Klimchouk, 1996a; Klimchouk *et al.*, 1996a; Johnson & Neal, 1997; Calaforra, 1998; Warren, 1999). Sauro (1996) indicated that medium-sized and large gypsum karst landforms, i.e. dolines, polje-like depressions, subsidence and collapse forms,

are similar in many respects to those found on carbonate karst. These features together with smaller scale, both dissolutional (pipes and cavities) and constructive (speleothems), forms in the gypsum host rock (Warren *et al*., 1990; Macaluso & Sauro, 1996) can remain preserved at the time the karst becomes inactive. Their preservation in the rock record is highly dependent on the evolutionary history of the basin in which the gypsum karst developed.

Palaeokarstic features recognized in gypsum formations originate mainly through intrastratal and/or interstratal dissolution, leading to a complex diagenetic pattern punctuated by multiple karst reactivations (Klimchouk, 1996a; Friedman, 1997). Distinction between palaeokarstic surfaces and subsurface or subjacent palaeokarst (Wright, 1982) is meaningful as the two types of palaeokarst provide very different information about the basin history. In particular, it is critical to ascertain whether solution took place at the atmosphere–rock interface, this representing a true surface palaeokarst, or developed after burial usually as a result of interstratal karst. Wright (1982) offered a set of simple criteria for recognizing surface-developed palaeokarstic surfaces from interstratal palaeo- or Recent karst. Examples of subsurface palaeokarsts in gypsum have been described by Cooper (1996) from Permian gypsum formations covered by Quaternary sediments in England, and by Andrejchuk (1996), who studied karstified Mesozoic gypsum buried by Neogene sediments in the pre-Urals region of Russia.

Gypsum palaeokarstic surfaces where solution features are well preserved have hardly been documented in the karst literature. This is probably the result of two factors (Klimchouk, 1996a): (1) the low preservation potential exhibited by gypsum karst especially when developed in non-marine successions; and (2) the difficulty of recognizing karst features in gypsum formations that have been subjected to strong changes under burial and/or have been pervasively weathered under subaerial exposure. Despite this, several case studies have documented palaeokarstic surfaces developed in gypsum formations both in Spain (Calvo *et al*., 1984; Armenteros *et al*., 1992; Rodríguez-Aranda *et al*., 1996; Cañaveras *et al*., 1996; Rodríguez-Aranda & Calvo, 1997) and abroad (Yaoru & Cooper, 1996; Friedman, 1997). The present study characterizes the petrology and sedimentology of a palaeokarst of Lower Miocene age developed in lacustrine gypsum deposits. Solution features and morphology of the palaeokarst surface are well preserved, which is rather uncommon in the rock record. The palaeokarstic surface is exposed in quarries where weathering has not obliterated the original karst features. Furthermore, burial did not reach more than 150 m; thus, the effect of burial diagenesis modifying primary mineralogy and textures is thought not to have been significant. Moreover, the palaeokarstic surface was sealed by fine-grained terrigenous deposits, which prevented later karst reactivation. The methods and terminology used in this study are quite similar to those for carbonate palaeokarsts (Wright, 1982, 1991; Esteban & Klappa, 1983; James & Choquette, 1988; Vanstone, 1998), although the peculiarities of gypsum karstification processes are outlined (Macaluso & Sauro, 1996; Klimchouk, 1996b; Klimchouk *et al*., 1996b; Calaforra, 1998).

GEOLOGICAL SETTING

The palaeokarst is located towards the upper part of the Tertiary succession of the Madrid Basin, a complex intracratonic basin in the centre of the Iberian Peninsula (Fig. 1) that reflects differences in the transmission of stresses from the active Iberian plate boundaries where the Betic and Pyrenean chains themselves had distinctive kinematic histories throughout the Tertiary (De Vicente *et al*., 1996). The complete succession ranges between 2000 and 3500 m in thickness, depending on the part of the basin (Calvo *et al*., 1996), and consists of both Palaeogene and Neogene terrestrial strata. The Neogene deposits have been divided stratigraphically into three main Miocene units and two Pliocene sedimentary cycles (Calvo *et al*., 1989), each separated by unconformities from the underlying units. In many cases, palaeokarsts occur in relation to those unconformities (Cañaveras *et al*., 1996; Sanz-Montero, 1996; Rodríguez-Aranda & Calvo, 1997).

The deposits of the Miocene Lower Unit, spanning Ramblian to Early Aragonian in age (Aquitanian–Burdigalian in the marine chronostratigraphic scale), lie horizontally across the basin, with the exception of the basin margin areas where they are affected by thrusts (eastern margin: Altomira Range) and reverse faults (northern and southern margins: Central System and Toledo Mountains; Figs 1 and 2). The Miocene Lower Unit comprises alluvial deposits that pass laterally into lacustrine evaporite sediments (Ordóñez *et al*., 1991). These deposits are

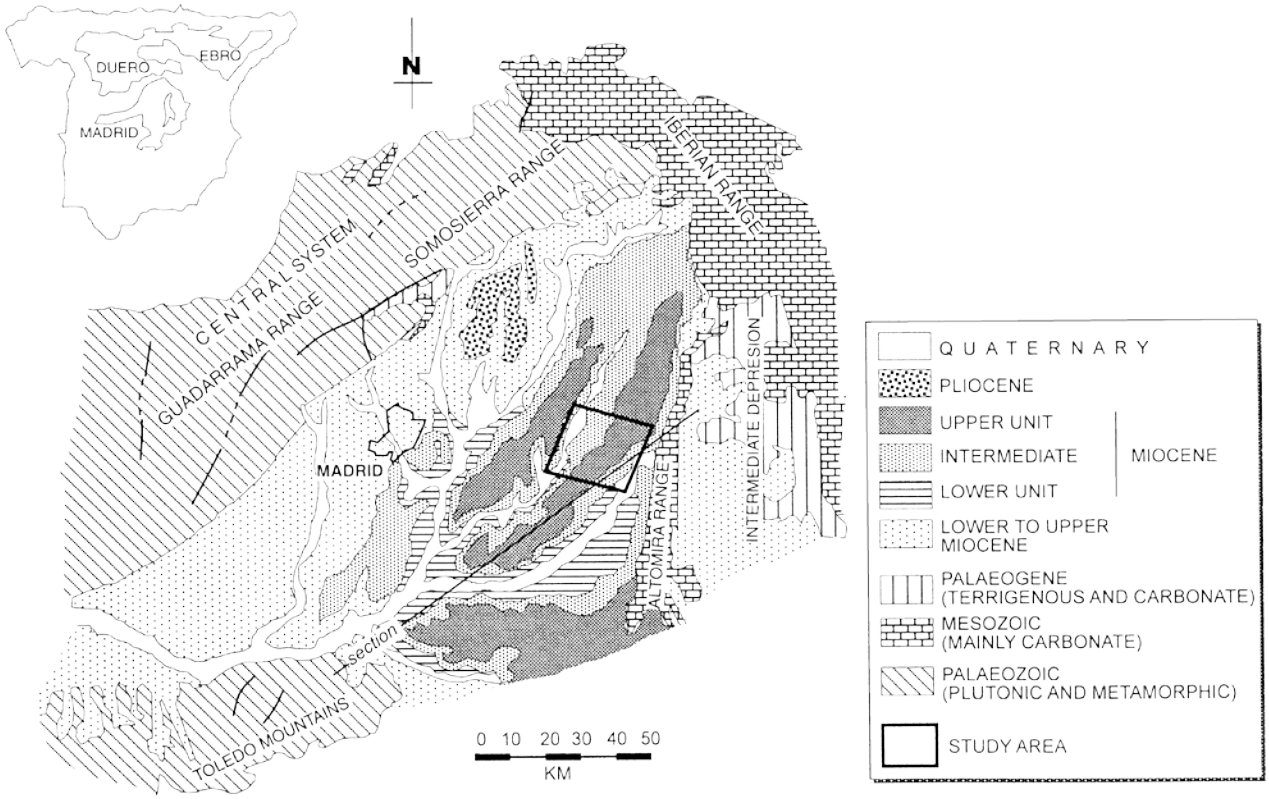

Fig. 1. Geological map of the Tertiary Madrid Basin showing location of the study area (boxed). Section line marks the profile shown in Fig. 2.

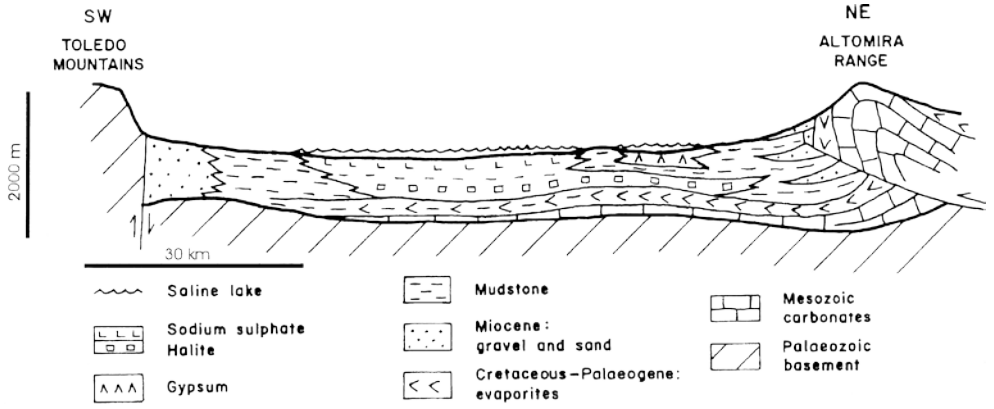

Fig. 2. Schematic stratigraphic section (see location in Fig. 1) showing the sedimentary fill of the Madrid Basin at the time when the Miocene Lower Unit was deposited. The study area corresponds to the small lake system filled with gypsum near the Altomira Range.

arranged according to a general concentric pattern, typical of a hydrologically closed saline lake basin (Hardie *et al.*, 1978). During the Lower Aragonian, several small saline lakes, ranging from 10 to 35 km in diameter, developed in the eastern part of the basin separated from a larger lake that occupied the basin centre (Fig. 2). In contrast to the variety of evaporite facies (halite, anhydrite, gypsum, thenardite and glauberite) recognized in the central lake, mainly gypsum accumulated in the small eastern lakes, perhaps because of more permanent drainage flows and further dilution of the lake waters in this part of the basin (Rodríguez-Aranda, 1995). The Miocene Intermediate Unit, from 50 to 200 m thick, spans the middle Aragonian to the early

Vallesian (Langhian to early Tortonian in the marine chronostratigraphic scale). It consists of a variety of alluvial and lacustrine deposits, which are arranged in a complex concentric pattern (Ordóñez *et al.*, 1991) characteristic of a lake basin that is both hydrologically and topographically closed. The lowermost deposits of the Miocene Intermediate Unit lie paraconformably on mudstones or on karstified gypsum deposits of the Lower Unit. These lowermost deposits consist of either terrigenous sediments or detrital gypsum depending on the part of the basin (Sanz *et al.*, 1994). In the study area, the Intermediate Unit begins with mudstone beds that overlie lacustrine gypsum deposits of the Lower Unit. Figure 3 shows a composite lithostratigraphic log of the main sedimentary units that crop out in the area.

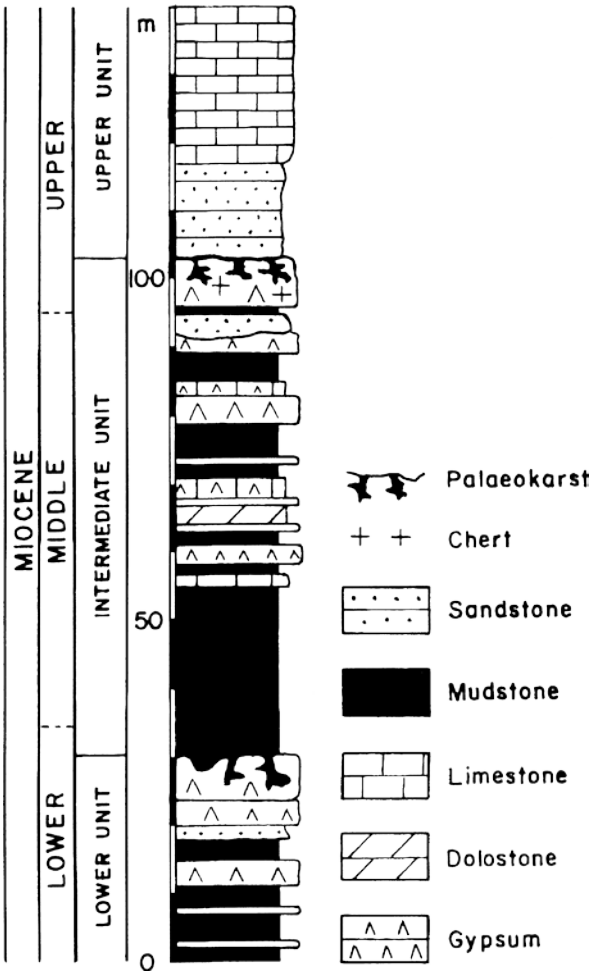

Fig. 3. Lithostratigraphic section of the Miocene in the study area. The gypsum palaeokarst studied in this paper is located towards the base of the section, defining the upper limit of the Miocene Lower Unit. A younger carbonate palaeokarst is located at the top of the Miocene Intermediate Unit where partly silicified gypsum deposits are covered by siliciclastic beds (Cañaveras *et al.*, 1996).

PALAEOKARSTIC FEATURES

Host rock

Description

The palaeokarstic surface is developed in a cream-coloured, up to 15 m thick tabular gypsum bed located at the top of the Miocene Lower Unit. The gypsum comprises 0Æ1 to 1 m thick beds of massive gypsum with interspersed centimetre-thick carbonate layers of peloidal dolomicrite in which charophyte stems and scattered gypsum lenses are locally observed. The gypsum consists of strongly bioturbated lenticular gypsum. Two main gypsum fabrics are distinguished:

1 Unimodal micro- to mesolenticular gypsum composed of untwinned, 0Æ025 to 0Æ3 mm-long lenses that commonly display syntaxial overgrowths. Clay and/or micrite matrix is absent or does not exceed 10% of the gypsum fabric (Fig. 4A).

2 Bimodal meso- to macrolenticular gypsum, similar to the fabric described above but including a population of larger, 0Æ5 to 5 mm long lenses of displacive and/or poikilotopic gypsum scattered within an aggregate of finer grained lenticular gypsum.

Both gypsum fabrics display pervasive bioturbation, usually exceeding 60% of the total bed volume, which is characterized by burrows of contorted morphologies tangled in all directions. The length of the individual burrows reaches up to 5 cm and ranges from 0Æ5 to 5 mm across. They typically show cylindrical meniscate backfill structures composed of micro- to mesolenticular gypsum (Fig. 4A). This type of burrowing structure has been defined as 'tangle-patterned small burrows' by Rodríguez-Aranda & Calvo (1998). In addition to this common burrowing structure, larger (up to 20 cm long, 0Æ5–3 cm across) isolated burrows, small (up to 7 cm long, 1–3 mm across) rhizoliths and a network of shafts and tunnels extending up to 1Æ5 m downward in the gypsum beds are recognized. The latter structure displays a branching pattern that resembles large root casts with diameters ranging from 2 to 20 cm. The infill of the tubes is passive and consists mainly of massive clay with variable amounts of carbonate and scattered gypsum lenses. Early diagenetic

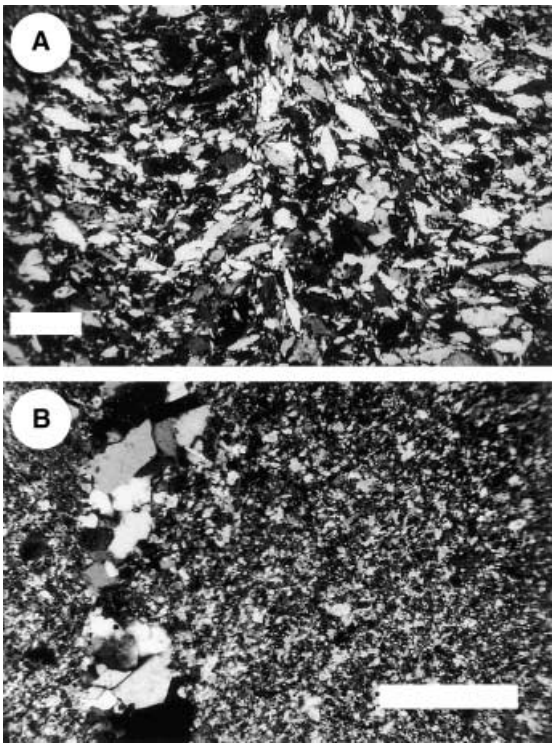

Fig. 4. Photomicrographs of the gypsum host rock. (A) Texture typical of primary unimodal mesolenticular gypsum showing meniscate backfill characteristic of tangle-patterned burrowing; scale bar ¼ 1 mm. (B) Anhedral microcrystalline gypsum mosaic resulting from early diagenetic transformation of lenticular gypsum; tubular structure at the left side of the photograph corresponds to a root hole cemented by mesocrystalline gypsum; scale bar ¼ 0Æ5 mm.

features, such as calcite nodules and patches of chert that mimic the burrow structures, are common within the gypsum.

In some places, the thickness of the gypsum is considerably reduced (up to 2 m) because of the combined effect of pinching out of the lake deposits towards the basin margin (Altomira Range) and karstification. The gypsum overlies red to green, massive and/or crudely laminated mudstone that locally behaved as a lower limit for dissolution.

Interpretation

The lenticular fabrics displayed by the gypsum correspond to primary gypsum deposited in an inland lake. The characteristic lens-shaped crystal morphology suggests the presence of trace amounts of continental organic matter (Cody, 1979; Cody & Cody, 1988) and high Ca^{2+}:$SO_4^{¼}$ ratios in the brine. The development of a population of larger displacive and/or poikilotopic crystal lenses reflects early diagenetic processes within the gypsum deposit. Extensive burrowing by dwelling fauna, tentatively attributed to subaquatic insect larvae of Chironomidae (Rodríguez-Aranda & Calvo, 1998), is indicative of moderate salinities and relatively low chlorinity (Rodríguez-Aranda & Calvo, 1998; Schreiber & El Tabakh, 2000). The presence of small rhizoliths is interpreted as a result of episodic plant colonization that probably represents short-term intervals of freshening, which is also supported by the occurrence of thin carbonate beds intercalated within the gypsum. Charophyte remains in the carbonate provide evidence of these episodes of lower salinity in the evaporite lake (Burne *et al.*, 1980). The networks of shafts and tunnels correspond to large rhizoliths probably associated with bushes. The pattern shown by the root branches seems to be typical of growth in a vadose environment (Cohen, 1982), and their sizes suggest that the growth of the bushes was particularly favoured during periods of low sedimentation rates. As discussed below, the abnormally large diameters (up to 20 cm) of some root casts are thought to have resulted from dissolutional enlargement related to karstification.

Sealing of the palaeokarstic surface

All across the area, the gypsum is overlain by clayey mudstone deposits that belong to the lowermost part of the Miocene Intermediate Unit (Fig. 3). These deposits, comprising green and reddish claystone, lie horizontally (Fig. 5) and range from 3 to 30 m in thickness. Intrasedimentary lenticular and rosette-like gypsum is commonly observed within the clayey mudstone. In addition, the mudstone displays root bioturbation, pedogenic carbonate beds and centimetre- to decimetre-thick intercalations of dolomicrite in which planar stromatolite structures are locally recognized. Clay mineralogy of the mudstone is dominated by illite with a low percentage (5–20%) of dioctahedral smectite. Quartz, calcite and dolomite are present in minor amounts within the clayey mudstone.

The contact between the mudstone and the underlying gypsum is sharp and defines a very irregular geometry characterized by residual blocks and depressions in which the clayey mudstone is accommodated usually as channel-like fills of variable extent. Locally, the clays infill conduits developed at the uppermost part of the underlying gypsum.

Fig. 5. Outcrop view of the gypsum palaeokarstic surface in a quarry located to the SW of the study area. The karstified gypsum, with a thickness of 3Æ5 m in the lower half of the photograph, shows a mammillated appearance looking rather like a boulder bed. The irregular upper surface of the gypsum is marked locally by residual blocks with steep walls (arrows). Note the sharp contact between the gypsum and the overlying, horizontally bedded mudstone that seals the palaeokarstic surface. One scour (s) filled up by siltstone and claystone with subordinate carbonate can be observed in the right side of the photograph.

Exokarstic (surface) features

Three main types of exokarstic features, i.e. small-scale solution features (karren), dolines and cylindrical pits, have been recognized (Fig. 6), all being characteristic of an epikarst (Ford & Williams, 1989). The description and classification of these features follow those used by Wright (1982, 1991), James & Choquette (1988) and Bosak *et al*. (1989) from carbonate palaeokarsts and Warren *et al*. (1990), Klimchouk (1996b), Sauro (1996) and Calaforra (1998) from recent gypsum karst. In the present study, the observations are obviously hindered by the fact that they can only be made in bidimensional views in quarry faces.

Besides the dissolution features, the gypsum host rock shows some alteration related to karstification, especially near the palaeokarst surface (Fig. 6), where it is seen as an irregularly shaped, centimetre- to decimetre-thick fringe characterized by orange to dark brown colours. Under the microscope, the altered gypsum typically exhibits anhedral micro- to mesocrystalline mosaics (Fig. 4B) containing some gypsum micronodules and ghosts of gypsum lenses. Anhydrite inclusions are often observed within the gypsum crystals. Root moulds that traverse the mosaics

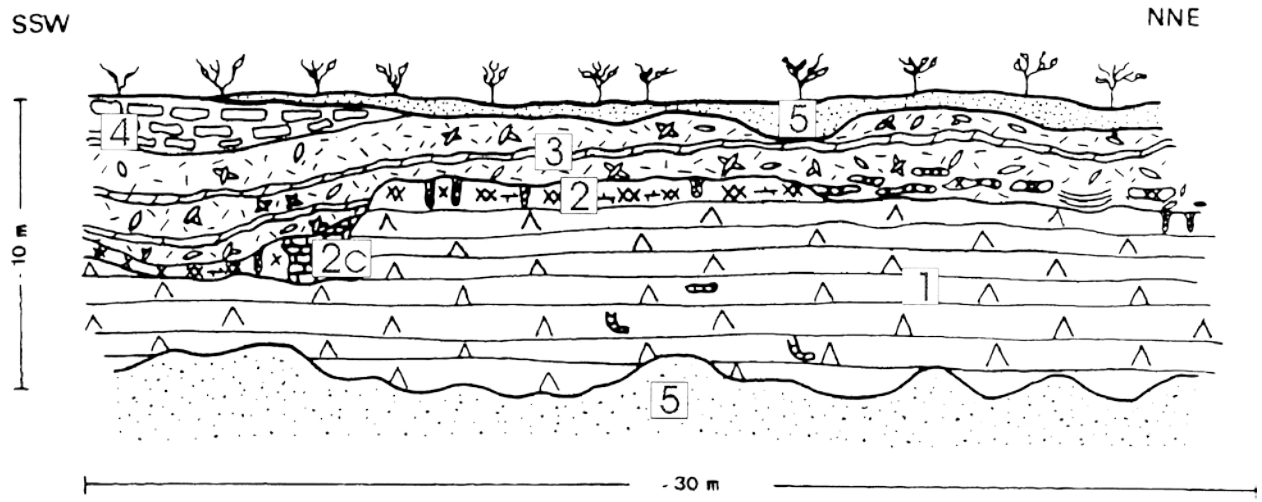

Fig. 6. Sketch showing the gypsum palaeokarstic surface in a quarry front near Pezuela de las Torres (SW of the study area). 1, Host rock (mainly bioturbated lenticular gypsum); 2, altered gypsum near the palaeokarstic surface; 2c, collapse structure containing carbonate breccia formed after replacement of gypsum blocks; 3, green and red claystone with lenticular gypsum and dolomicrite beds; 4, boxwork limestone; 5, recent soil and colluvium.

vertically and are cemented by gypsum are present locally (Fig. 4B).

Small-scale solution features

Small-scale solution features comprise several morphologies that can be integrated under the generic name of 'karren' (Bögli, 1980). These forms consist of small- to medium-scale scours, up to 1Æ5 m in width and a few decimetres in depth, which display smoothed asymmetrical sides and a concave-upward geometry. Some scours exhibit a central incision at the lowermost part of the concave surface. Although only observed in cross-section, it seems that the axes of the scours are not preferentially aligned and do not follow a definite pattern. Lapies morphologies, which are commonly preserved in carbonate karsts (Esteban & Klappa, 1983), have not been recognized clearly in the gypsum palaeokarst, probably because of reworking and further smoothing of the gypsum surfaces.

The scours are typically filled by trough cross-laminated siltstone (Fig. 5) that is locally interbedded with centimetre-thick planar stromatolites.

These forms can tentatively be classified as typical of a meander karren (*sensu* Bögli, 1980). This type of karren is rarely developed in carbonate rocks subjected to karstification (Ford & Williams, 1989), but is common in gypsum rocks where the gradient for water flow is very low (Calaforra, 1998). In this case, the scours possibly behaved as small channels that fed sinks and dolines developed in the karst surface.

Dolines

In the quarry faces, dolines are seen as depressions of variable size (Fig. 6), not exceeding 15 m in width and up to 2 m in depth (usually the width:depth ratio is more than 3). The walls of the dolines are frequently asymmetrical; one wall is steep and the other one is gentle. The floors of the dolines display a concave-up or flat geometry, the latter case being coincident with the bedding of the gypsum host rock. Locally, the floors are veneered by thin collapse breccia and/or exhibit vertical conduits containing massive claystone at the bottom of the depressions.

The dolines are filled by green and/or reddish clayey mudstone showing relatively abundant root bioturbation and scattered gypsum lenses and/or rosette-like gypsum aggregates. Sandstone formed of detrital gypsum grains is locally present as a sedimentary fill of the dolines. Tabular to lensoidal, 10 to 40 cm thick carbonate beds are locally intercalated in the clays, thinning and pinching out against the walls of the dolines (Fig. 7A). The carbonate consists of massive to peloidal dolomicrite and/or white carbonate nodules showing pedogenic features such as laminar coatings and pisoids. Fault planes outlined by satin-spar gypsum are commonly recognized within the claystone fill of the dolines (Fig. 7A). In other cases, the sedimentary fill of the dolines consists of clayey mudstone beds that maintain their thickness and show an abrupt lateral contact with the doline wall (Fig. 7B). The former case is considered to be indicative of pre- and/or syn-sedimentary fill accompanying karstic dissolution of the gypsum substrate that resulted in the deepening of the doline. The latter case represents a post-sedimentary fill of the dolines, as a depression existed before the fine-grained deposit spread out on the palaeokarstic surface.

This pattern of co-existing pre- or syndepositional fills and post-depositional sediment accumulation in dolines has been observed in other geological situations where a sedimentary formation covers a dissolutional and/or erosional surface sculpted in soluble rocks (Halfar *et al*., 1998). As pointed out by Klimchouk (1996b), dissolution processes in gypsum are quite effective even in places where the gypsum substrate is overlain by stagnant water.

Cylindrical and funnel-shaped pits

Up to 1 m deep and 10 to 30 cm wide pits are observed across the karstified gypsum surface (Fig. 8A and B). The pits are either cylindrical or funnel shaped (*sensu* Vanstone, 1998), and are interspersed with areas of relatively bare gypsum pavement. Cylindrical pits exhibit a narrow tubular form (Fig. 8A) with irregular walls that show local horizontal branching, the individual branches being centimetric in diameter. Usually, the walls are veneered by up to 1 cm thick satin-spar gypsum crusts. The fill of the pits consists mainly of claystone, although aggregates of macrocrystalline gypsum are commonly recognized, especially in the upper parts of the pits. The pits taper sharply downward. Funnel-shaped pits comprise cylindrical pits in which the upper portion of the pit wall is bevelled and slopes smoothly inwards (Fig. 8B). Maximum observed diameter of the funnels is 30 cm. Similar to the cylindrical pits, gypsum veneers and claystone fills characterize the funnel-shaped pits.

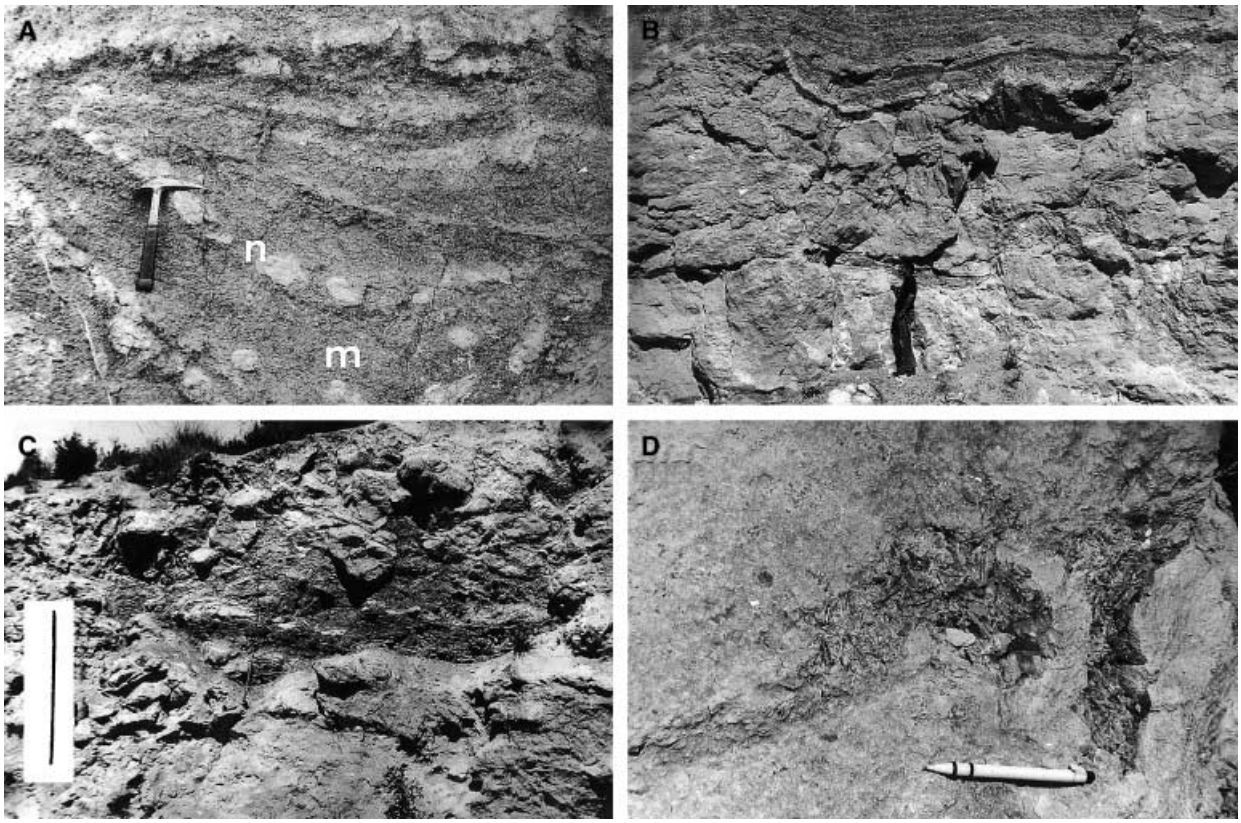

Fig. 7. Features of the gypsum palaeokarst. (A) Sedimentary fill of a doline containing clayey mudstone (m) with intercalated carbonate beds and nodules (n); beds pinch out near the walls of the doline; local fault planes are filled by satin-spar gypsum (f); hammer for scale. (B) View of a doline filled by claystone (upper part of the photograph) that onlaps against the gypsum walls (right side of the picture); horizontal caves filled by clays (arrowed) occur aligned 2 m below the floor of the doline; person for scale. (C) Large cave filled with green clayey mudstone and white carbonate beds. Scale bar ¼ 2 m. (D) Conduits cemented by macrocrystalline gypsum. Note a section with T morphology on the right. Pencil for scale ¼ 14 cm.

Both the geometries of the pits and the presence of branching forms suggest that they were related to penetration of roots, probably from bushes that grew scattered on the gypsum surface (Rodríguez-Aranda *et al.*, 1996; Rodríguez-Aranda & Calvo, 1998). This is in agreement with Gunatilaka (1990), who observed the presence of plants in supratidal sabkhas of the Arabian Gulf and their role in the early transformation of primary gypsum to anhydrite. Vanstone (1998) has described and discussed in detail the formation of palaeokarst pits developed in Late Dinantian exposure surfaces from southern Great Britain. His conclusion is that the pits did not form through direct root action, that is they do not represent root casts or rhizocretions (Klappa, 1980), but resulted from initial stem-flow drainage from trees driving the percolation of acidic soil water, which was followed downwards by dissolution enlargement of the root traces (Vanstone, 1998). This model of pit formation can explain the presence of cylindrical and funnel-shaped pits in the gypsum palaeokarstic surface of Madrid. There, the diameters of the vertical conduits are obviously too large to represent root casts directly and features related to roots are not preserved. In the present case, however, the initiation of the pits probably occurred after plant decay in a lithified gypsum ground. Accordingly, the roots behaved simply as a pathway for the percolation of water, resulting in progressive enlargement by gypsum dissolution and further passive filling and cementation of the pit walls (Rodríguez-Aranda & Calvo, 1998).

Endokarstic (subsurface) features

The Lower Miocene gypsum palaeokarst is characterized by a rather complex network of horizontally elongated to pocket-like caves connected by vertical to oblique irregular conduits. In addition, collapse breccias are recognized locally across the karst profile (Fig. 6).

Fig. 8. (A) Outcrop view of a cylindrical pit; note the irregular form of the pit walls that show local lateral branching. (B) Close-up view of a funnel developed in the upper portion of a pit. Pencil for scale is 14 cm long.

Caves and conduits

These forms are especially well developed in places where the karst profile exceeds 2 m in depth. Horizontal caves, usually filled with clayey mudstone (Fig. 7C), occur aligned at variable depths, ranging from 2Æ5 to 3Æ5 m, beneath the palaeokarst surface. Most common cave dimensions are in the range from 2 to 3 m in width and from 0Æ20 to 0Æ40 m in height. Some larger caves, reaching up to 8 m in width and 2 m in height, are locally recognized. The caves have concave floors and irregular roofs, although the initial morphology was slightly modified by later compaction. The sedimentary fill of the caves consists mainly of green, roughly laminated clays containing plant remains and showing oxidized surfaces. In the larger caves, the sedimentary fill is more complex and comprises, from bottom to top, green laminated claystone with intervening carbonate, followed by massive green clayey mudstone in which disseminated calcite rafts and patches of reworked calcitized gypsum are common. Intrasedimentary gypsum crystals also occur dispersed in this sediment.

Vertical conduits, filled with green clayey mudstone and gypsum clasts, connect the upper surface of the caves to the palaeokarst surface. The conduits are usually 10–30 cm wide, and their length varies with the depth at which the caves are located. In some cases, conduits that do not show connection to the palaeokarst surface are observed. These latter conduits display either elliptical geometries, T-shaped (Fig. 7D) or key-hole forms (Ford, 1988), with diameters ranging from 2 to 10 cm and lengths of up to 1 m. The sedimentary fill of these conduits consists mainly of macrocrystalline (centimetre-sized) gypsum with variable amounts of clays. Crusts of satin-spar gypsum occur locally associated with the conduits.

The distribution of caves and conduits in the gypsum and their proximity to the karstic surface suggest that dissolution took place in an unconfined aquifer where the caves were hydraulically interconnected. In this setting, the water table is under atmospheric pressure and is free to rise and fall after water recharge of the aquifer, causing variation in the phreatic and vadose zones (Klimchouk, 1996b). The preservation of large caves at shallow depths is unusual and, in the present case, can be explained by the ‘paragenetic’ pattern proposed by Ford & Williams (1989). According to this pattern, burial of the cave floors by clay pushes the solutional attack outwards and upwards, thus contributing to the stability of the mechanically weak gypsum strata.

The dominant horizontal, lens-shaped morphology of the caves and their occurrence at relatively fixed depth argue for development of the caves in relation to the fluctuation of the water table, that is the caves were not restricted to the phreatic zone. This is supported by the presence of T-shaped conduits above the caves, a morphology that is thought to develop typically in the vadose zone (Thraikill, 1968; Ford, 1988).

Collapse breccias

Collapse breccias consist of silt- to boulder-sized, subrounded clasts of gypsum embedded with clay and/or carbonate, which occur locally at the bottom of some dolines. In cross-section, the breccias are up to 2 m wide and 2Æ5 m thick pocket-like deposits (Figs 5 and 6). The gypsum clasts are partly or totally replaced by carbonate, resulting in pieces of boxwork calcite characterized by gypsum pseudomorphs and abundant

open moldic porosity. The collapse breccias are interpreted as a result of localized gravitational breakdown and crumbling of underlying caves, the process being triggered by erosion, dissolution and subsequent mechanical instability of cave walls and ceilings under stress from the weight of overlying strata. The reduced extent of the collapse breccia deposits is in contrast to those developed largely in karstified carbonate formations (Loucks, 1999). Moreover, the size of the collapse breccias from the Miocene palaeokarst of the Madrid Basin is out of the range of many other collapse breccias formed by dissolution-collapse of evaporites where the evaporites are associated with carbonate (Friedman, 1997; Warren, 1999). In the present case, the formation of the breccias relates to relatively small caves, and the lowering of the cave walls and ceilings may have been gradual, the two factors preventing sudden collapse of the overlying strata.

Replacement of gypsum breccia clasts by calcite suggests that the deposit evolved under the influence of meteoric water. The reaction involves dissolution of the calcium sulphate by bicarbonate-bearing water in which the bicarbonate ions are derived from the dissolved CO_2 as a product of the oxidation of organic compounds of terrestrial origin (Pierre & Rouchy, 1988).

EVOLUTION OF THE GYPSUM PALAEOKARST

The palaeokarst began to form after the saline lake basin in which extensive layered gypsum deposits were accumulated dried up. This is supported by the presence of cylindrical and funnel-shaped pits, which are interpreted to result from the penetration of the roots of small trees and/or bushes that grew sparsely on the desiccated lake bed. The root holes acted as preferential pathways for percolation of water, causing enlargement by dissolution of the gypsum and further formation of conduits and caves that were connected to the gypsum surface. This pattern fits well with that of an exposed karst (Wright, 1982; Warren *et al*., 1990; Klimchouk, 1996a), where an areally uniform denudational surface of a gypsum formation is directly exposed to aggressive meteoric waters causing a great variety of dissolution-sculpted landforms.

Detailed descriptions and interpretations of exposed gypsum palaeokarsts are not common in the sedimentological literature. Yaoru & Cooper (1996) described a large palaeokarst developed in gypsum, associated with mudstone and dolomite, of the Ordovician Fenfeng Formation in central China. This palaeokarst shows collapse columns and breccia pipes reaching up to several tens of metres in thickness, the palaeokarstic surface being covered by Carboniferous strata. Friedman (1997) described several case studies of palaeokarst developed in evaporites from Lower Palaeozoic terranes of North America. In Spain, gypsum palaeokarstic surfaces similar to that of the Madrid Basin have been recognized in Middle Miocene formations of the Duero Basin (Armenteros *et al*., 1992) and Upper Miocene gypsum deposits of the Betic area (Bustillo *et al*., 2000).

Initiation of the palaeokarst

The accumulation of the lenticular gypsum deposits in which the palaeokarst developed took place in a shallow saline lake (Rodríguez-Aranda, 1995; Rodríguez-Aranda & Calvo, 1998). Gypsum, with a small amount of clay and carbonate, was the dominant evaporite mineral in the lake sediments. The gypsum displays a typical sedimentary fabric characterized by extensive burrowing, which is interpreted as mainly the result of feeding and/or dwelling activity of chironomids (Rodríguez-Aranda & Calvo, 1998). These organisms are organic detritus feeders that can develop dense populations in permanently or episodically submerged environments (De Deckker, 1988). This bioturbated lenticular gypsum has been interpreted as typical of moderately saline lake conditions, as chironomids tolerate a rather broad range of salinity (70–170 g $L^{)1}$; Hammer, 1986).

Examples of early karstification processes in modern evaporite settings

Recognition of modern saline lake environments, such as Lake Amadeus in central Australia (Chen *et al*., 1991) and saline lakes of the northern Great Plains of western Canada (Powers & Hassinger, 1985; Last, 1993), provides evidence that gypsum and other evaporite minerals, e.g. halite, can be strongly indurated at the time at which the lakes dry up. In these settings, the lake deposits can be subjected to episodic freshening that results in large- to medium-scale dissolutional features. In addition, Yaoru & Cooper (1996) have reported the occurrence of relic lake basins in north-west China (e.g. the Chaidamu Basin), where gypsum deposits of Pleistocene age have developed karst features including corroded flutes, fissures, small

caves and associated collapses. Moreover, the role of halophyte plants in fissuring and promoting diagenetic transformation of saline grounds has been pointed out by Gunatilaka (1990) from sabkhas of the Arabian Gulf. In her case study, Gunatilaka (1990) observed that an indurated gypsum crust is formed in the vadose zone of the sabkha as a result of transformation of primary gypsum to anhydrite, a process driven by the presence of halophytic plants (Gunatilaka *et al*., 1980). On the death of the plants, the anhydrite is hydrated back to gypsum.

Model for the initiation of the palaeokarst

The aforementioned mechanisms of gypsum ground formation are envisaged as a reliable model to explain the initiation of the gypsum palaeokarst in Madrid, as it displays several features (i.e. anhydrite inclusions in the gypsum crystals, alteration of the primary lenticular gypsum into micro- to mesocrystalline mosaics, remains of plant roots converted to karst pits) similar to those observed in recent environments where saline lakes become dried up. The proposed model (Fig. 9) includes several successive stages. Stage 1 represents the accumulation and bioturbation of lenticular gypsum in a moderately saline lake. After drying up of the lake, the poorly indurated gypsum ground was colonized by plants (Stage 2). In this setting, halophytic plants could contribute to the local transformation of primary lenticular gypsum to anhydrite through a dissolution–reprecipitation process, similar to that reported from vadose zones in supratidal sabkhas (Gunatilaka, 1990). Stage 3 corresponds to the death and decay of plants, the root holes behaving as initial conduits for meteoric water percolation and/or alteration of the saline ground, this becoming progressively indurated (Fig. 9). Under these conditions, anhydrite formed in close relationship with plants is unstable and is transformed to secondary gypsum.

Development and maturation of the karst profile

Enlargement by dissolution of the initial conduits (Stage 4 in Fig. 9) resulted in the formation

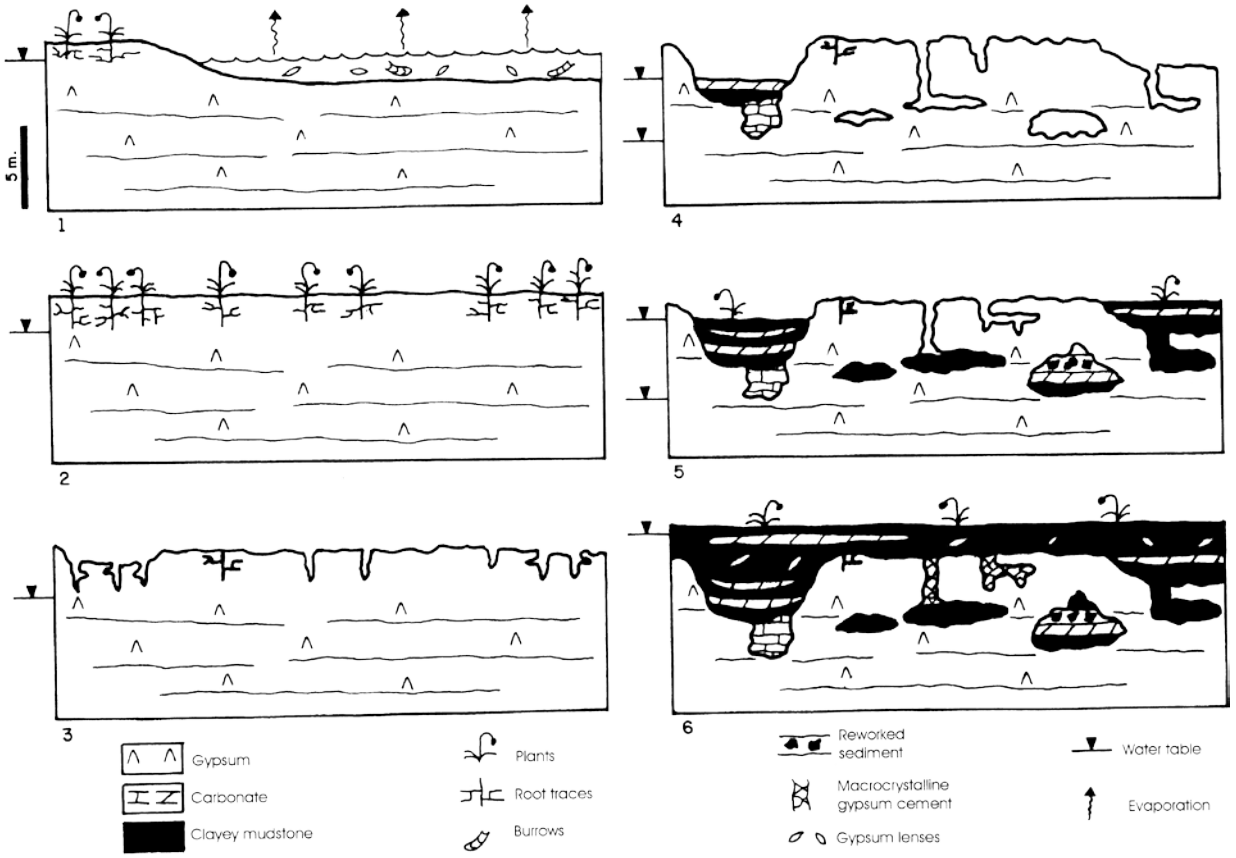

Fig. 9. Idealized sketch model for the initiation (stages 1–3), maturation (stages 4 and 5) and preservation (stage 6) of the gypsum palaeokarst. See text for explanation.

of cylindrical and funnel-shaped pits that mimic, but do not strictly represent, root casts or rhizocretions. The observation of the palaeokarst surface suggests that the pits were not densely packed. Formation of the dolines was probably favoured by lateral amalgamation of adjacent pits, ultimately related to colonization by closely spaced bushes. This could create local areas in which the gypsum substrate was breached by the development of a relatively denser network of plant roots, resulting in more extensive drainage and further dissolution of the gypsum ground.

Factors limiting downward development of the karst features

Both conduits and caves reach only up to a few metres below the palaeokarst surface. This suggests that there were some factors limiting downward propagation of dissolution within the gypsum substrate. The influence of a shallow water table during the development of the karst is envisaged as a critical factor that limited the depth reached by both exokarst and endokarst features (Figs 6 and 9). In addition, the formation of roughly planar, horizontal cavities is probably related to the top of the water table, which represents the maximum depth for root penetration (Fig. 9, stage 4).

The formation of the horizontal caves could also be constrained by stratification planes in the gypsum host rock. The discontinuities between gypsum beds probably acted as preferential flow paths in which groundwater became increasingly saturated in sulphate. Considering the subhorizontal geometry of the Miocene gypsum strata and the fact that the unit does not exhibit significant fracturing, the initiation of the caves probably took place under low groundwater flow rates. The enlargement of the caves may have been accelerated by water flowing downwards through the vertical conduits that connected the caves to the karst surface. As noted by several authors working in karst of modern semi-arid regions (Klimchouk, 1996b; Calaforra, 1998), water discharge through karst conduits is discontinuous and controlled by episodic heavy rainfall events in this climatic setting. Under these conditions, most active conduits enlarge rapidly to accommodate the highest possible discharge (Forti, 1993) and, thus, episodic water flows can easily reach the lower karst levels, contributing to cave development.

Processes derived from fast dissolution rates of gypsum

The enlargement of conduits and caves within the palaeokarst profile was favoured by fast dissolution kinetics of the gypsum. The solubility of gypsum in pure water is roughly 10–20 times greater than the solubility of calcite in the presence of CO_2, and the influence of temperature on gypsum solubility is minor (Klimchouk, 1996b). Thus, the development of the gypsum karst system could have been rapid, even though the initial openings were small (<10 lm to 1 mm; Ford & Williams, 1989). Local water seepage through these small holes is thought to have been slow and laminar, but rapid dissolution of gypsum would result in widening and the development of more turbulent flows. As pointed out by Klimchouk (1996b), this accelerated dissolution process implies rapid increase of solute concentration to near gypsum saturation level, which makes quite effective the dissolutional enlargement of the initial caves and allows a higher penetration of significantly undersaturated water beyond the end of the caves.

Moreover, dissolution in the aerated zone of exposed karst massifs can be notably enhanced by condensation processes, especially in karsts of semi-arid regions (Forti, 1993; Calaforra, 1998). Condensation water formed by differences in temperature between the outside and in-cave atmospheres is very aggressive and causes substantial dissolution that, added to gypsum's high solubility and fast dissolution kinetics, would result in rapid enlargement of conduits and caves throughout the gypsum karst profile.

Synsedimentary fill of the karst system

Formation of conduits and caves was coeval with the development of dolines, and all these features contain partial sedimentary fills of clayey mudstone, carbonate and detrital gypsum (Fig. 9, stage 5). The origin of the clays, occurring mainly as roughly laminated, green clayey mudstone beds, is uncertain, although they could be reworked from mudflat and alluvial fan deposits that are laterally associated with the lacustrine gypsum (Rodríguez-Aranda, 1995). The accumulation of clay was probably related to periodic flooding of the karstified surface, where the caves and doline floors were favourable zones for ponding of waters containing a relatively high concentration of suspended

fine-grained siliciclastic material and organic detritus. These mudstone fills are similar to the mud-filled cavities observed by Last (1993) in saline lakes of the northern Great Plains of western Canada, and are consistent with the episodic clastic input pattern recognized by Calaforra (1998) in the gypsum karst system of the Sorbas Basin, SE Spain, developed under semi-arid to arid climatic conditions. In this setting, clastic input is highly dependent on very episodic heavy rainfall that, in turn, helps to erode the gypsum walls, resulting in the deposition of detrital gypsum interbedded and/or mixed with the clay.

Carbonate is present in the sedimentary fill of both dolines and caves throughout the karst profiles. However, carbonate in the dolines consists of massive to peloidal dolomicrite or nodules developed in laminated claystone, whereas the carbonate found in caves commonly consists of calcite rafts and patches of reworked calcitized gypsum. The doline carbonates were probably deposited in shallow water that was episodically ponded in the karstic depressions, whereas the carbonate nodules probably formed pedogenically in clays, thus supporting a punctuated regime for the sedimentary fill of the dolines. As discussed above, the lateral thinning of the clays and associated carbonates towards the walls of the dolines (Fig. 7A) provides evidence that their accumulation took place at the same time as dissolution of the gypsum floor.

The occurrence of calcite rafts in the clayey cave deposits suggests that input of clastic sediment alternated with periods of standing water. Calcite rafts have been recognized as a relatively common carbonate precipitate forming at the air–water interface of pools in caves (Pomar *et al*., 1976; Hill & Forti, 1977; Esteban & Klappa, 1983). In this setting, where gypsum supplies a large excess of Ca ions to the cave ponds, formation of the calcite rafts resulted from evaporation, which enriches the Ca^{2+} ion content in the standing water, causing precipitation onto dust grains floating on the meniscus (Hill & Forti, 1977).

The reworked calcitized gypsum originated either as simple gypsum clasts that were introduced into the caves by episodic flooding and then calcitized under the influence of meteoric water, or as fragments of previously replaced gypsum fallen from the cave walls and ceilings. No definitive evidence was found to support either mechanism. In either case, calcitization of gypsum by meteoric water is the most likely mechanism for the partial or total replacement of gypsum clasts by carbonate in the collapse breccias (see discussion above). This mechanism has been demonstrated to be effective in other evaporite formations showing extensive calcitization (e.g. the Miocene Calatayud Basin of NE Spain; Sanz-Rubio *et al*., 2001).

Preservation of the gypsum palaeokarst

In all studied quarries, the gypsum palaeokarst surface is covered by crudely laminated clayey mudstone deposits, with intervening carbonate and intrasedimentary gypsum, that lie horizontally bedded (Figs 3 and 5). These overlying deposits, interpreted as distal mudflat facies of alluvial systems coming from the north and east of the basin (Rodríguez-Aranda, 1995; Rodríguez-Aranda & Calvo, 1997), do not show any evidence of collapse into the palaeokarstic surface. This clearly indicates that gypsum dissolution did not continue after deposition of the alluvial sediments, and that the deposits preserved the palaeokarstic surface at the time at which the karst system became inactive.

Given the irregularities of the exposed palaeokarstic surface, i.e. doline depressions and unfilled cavities (pits and conduits), the overlying alluvial sediments accumulated following the karst morphology (Fig. 9, stage 6). Thus, dolines provided some accommodation space for the accumulation of clayey mudstone beds that lie unconformably over the synsedimentary fill of the depressions (Fig. 7A) and, in turn, show an abrupt lateral contact with the doline walls (Fig. 7B). After the dolines were entirely filled by fine-grained sediment, this covered the adjacent top surface clearly defining a sedimentary discontinuity between the gypsum and the clay.

Clays also accumulated in pits and conduits that were not filled in the former stages of karstification, especially in those cavities that underwent substantial solution enlargement. The infill of the cavities included gypsum cementation that completely filled the created porosity (Fig. 7D). This cementation consists of rather homogeneous mosaics of macrocrystalline gypsum (Fig. 9, stage 6), and is interpreted as having been developed under phreatic conditions, consistent with a rise in the water table that accompanied the deposition of the terrigenous sediments that seal the palaeokarstic surface.

DISCUSSION AND CONCLUDING REMARKS

The gypsum palaeokarst can be characterized as an uncovered karst, i.e. formed at the atmosphere–rock interface (Wright, 1982), which resulted in a palaeokarstic surface with associated and relatively well-developed subsurface karst features (caves and internal conduits). The features observed correspond to a well-preserved gypsum epikarst assemblage. The palaeokarstic surface marks a regional stratigraphic discontinuity that was buried by terrestrial deposits, related to a generalized progradation of alluvial systems (Ordóñez *et al*., 1991) that preserved the karstified surface. The overlying deposits do not show any evidence of collapse into the underlying surface, which indicates that solution did not continue after burial.

Both the vertical extent of conduits and the depth of caves within the karst profile are consistent with the influence of a shallow water table during development. However, the inferred palaeowater table was probably positioned at different levels in the gypsum host rock (Fig. 9). A low hydraulic gradient is assumed for the formation of the karst in view of the flat or extremely gently dipping geometry of the gypsum stratigraphic unit at the time at which the palaeokarst developed (Rodríguez-Aranda, 1995).

The development of the gypsum palaeokarst took place under a semi-arid to arid climate, which is in agreement with the evolutionary climatic pattern deduced for the Lower to Middle Miocene sedimentary record of the Madrid Basin (Calvo *et al*., 1996). Modern examples of gypsum karst in semi-arid to arid settings, such as those from exposed Permian gypsum formations of New Mexico (Peerman & Belski, 1991), Neogene gypsum of central Sicily (Agnesi *et al*., 1985) and Messinian gypsum of SE Spain (Calaforra, 1998), indicate that the evolution of the karst morphology and associated products is highly dependent upon the temperature and rainfall regime, the latter usually being related to episodic heavy rainfall discharges. Dissolutional and/or mechanical denudation rates estimated by different techniques in these gypsum karst systems, i.e. tablet weight loss, determinations of solute loads (Klimchouk *et al*., 1996b; Calaforra, 1998), range from 0Æ3 mm year^{-1} in external parts of the karsts to 0Æ03 mm year^{-1} in caves and other internal conduits. These average denudation rates are considerably greater than those estimated for karstified carbonate formations (Klimchouk *et al*., 1996b). Moreover, dissolutional denudation is considered to be much more important than mechanical erosion in gypsum formations subjected to karstification (Calaforra, 1998), which is in agreement with the limited occurrence of detrital gypsum deposits in both exo- and endokarstic zones of the Miocene palaeokarst in the Madrid Basin.

Duration of karstification is estimated to have been short, probably representing hundreds or a few thousands of years. This estimation is supported by the high solution rates characteristic of shallow epikarst aquifers in gypsum formations, especially where the karst forms under semi-arid to arid conditions (Ford & Williams, 1989), and is consistent with the findings of Klimchouk (1996b) and Johnson & Neal (1997) that gypsum karstification can develop rapidly over geologically short time periods. High dissolution rates of gypsum would account for the short duration of the karstification, which is in contrast to longer durations estimated for the development of carbonate palaeokarsts (Esteban, 1991).

ACKNOWLEDGEMENTS

This paper has benefited from extensive regional work and fruitful discussions with Drs Salvador Ordóñez (University of Alicante) and Jean Marie Rouchy (Laboratoire de Geologie, Muséum National d'Histoire Naturelle de Paris). We are grateful to Drs José M. Calaforra (University of Almería) and Francisco Gutiérrez (University of Zaragoza) for their valuable comments on the geological behaviour of recent gypsum karsts. We acknowledge constructive reviews by Derek Ford and Peter Mozley. Thanks are also given to Dr Pablo Peláez and Jesús Sánchez for technical assistance with drawings and photographs. The study was supported financially by the Spanish Ministry of Teaching and Culture through several projects developed in recent years.

REFERENCES

Agnesi, V., Macaluso, T., Madonia, P., Montoro, M., Panzica, M., Pipitone, G. and Ramberti, L. (1985) *Evaporite Karst in Sicily*. International Symposium on Evaporite Karst, Field-trip Guidebook, 28 pp.

Andrejchuk, V. (1996) Gypsum karst in the pre-Ural region, Russia. In: *Gypsum Karsts of the World* (Eds A. Klimchouk, D. Lowe, A. Cooper and U. Sauro), *Int. J. Speleol*., 25, 285–292.

Armenteros, I., Blanco, J.A. and Hervalejo, M.V. (1992) Sedimentación continental miocena y procesos diagenéticos en la Cuenca de Sacramenia-Fuentidueña, Cuenca del Duero. In: *Guía de las Excursiones Geológicas del III Congreso Geológico de España, Salamanca* (Eds J.J. Durán and A. Carnicero), pp. 290–299.

Bögli, A. (1980) *Karst Hydrology and Physical Speleology*. Springer-Verlag, Berlin, 203 pp.

Bosak, P., Ford, D.C., Glazek, J. and Horacek, I. (Eds) (1989) *Paleokarst. A systematic and regional review*. Elsevier, Amsterdam, 725 pp.

Burne, R.V., Bauld, J. and DeDeckker, P. (1980) Saline lake charophytes and their geological significance. *J. Sed. Petrol*., 50, 281–293.

Bustillo, M.A., Arias, C. and Vilas, L. (2000) Silicificación y paleokarstificación en depósitos evaporíticos continentales (Hoya de la Sima, Jumilla). *Geotemas*, I, 209–212.

Calaforra, J.M. (1998) *Karstología de Yesos*. Serv. Publ. Univ. Almería, Spain. Monografía Ciencia y Tecnología, 3, 384 pp.

Calvo, J.P., Ordóñez, S. and García del Cura, M.A. (1984) Caracterización sedimentológica de la Unidad Intermedia del Mioceno en la zona sur de Madrid. *Rev. Mat. Proc. Geol*., 2, 145–176.

Calvo, J.P., Ordóñez, S., García del Cura, M.A., Hoyos, M. and Alonso Zarza, A.M. (1989) Sedimentología de los complejos lacustres miocenos de la Cuenca de Madrid. *Acta Geol. Hisp*., 24, 281–294.

Calvo, J.P., Alonso Zarza, A.M., García del Cura, M.A., Ordóñez, S., Rodríguez-Aranda, J.P. and Sanz Montero, M.E. (1996) Sedimentary evolution of lake systems through the Miocene of the Madrid Basin: paleoclimatic and paleohydrological constraints. In: *Tertiary Basins of Spain. The Stratigraphic Record of Crustal Kinematics* (Eds P.F. Friend and C.J. Dabrio), pp. 272–277. Cambridge University Press, Cambridge.

Cañaveras, J.C., Calvo, J.P., Hoyos, M. and Ordóñez, S. (1996) Paleomorphologic features of an intra-Vallesian paleokarst, Tertiary Madrid Basin: significance of paleokarstic surfaces in continental basin analysis. In: *Tertiary Basins of Spain. The Stratigraphic Record of Crustal Kinematics* (Eds P.F. Friend and C.J. Dabrio), pp. 278–284. Cambridge University Press, Cambridge.

Chen, X.Y., Bowler, J.M. and Magee, J.W. (1991) Aeolian landscapes in central Australia: gypsiferous and quartz dune environments from Lake Amadeus. *Sedimentology*, 38, 519–538.

Cody, R.D. (1979) Lenticular gypsum: occurrences in nature, and experimental determinations of soluble green plant material on its formation. *J. Sed. Petrol*., 49, 1015–1028.

Cody, R.D. and Cody, A.M. (1988) Gypsum nucleation on crystal morphology in analog saline terrestrial environments. *J. Sed. Petrol*., 58, 247–255.

Cohen, A. (1982) Paleoenvironments of root casts from the Koobi Fora Formation, Kenya. *J. Sed. Petrol*., 52, 401–414.

Cooper, A. (1996) Gypsum karst of Great Britain. In: *Gypsum Karsts of the World* (Eds A. Klimchouk, D. Lowe, A. Cooper and U. Sauro), *Int. J. Speleol*., 25, 195–202.

De Deckker, P. (1988) Biological and sedimentary facies of Australian salt lakes. *Palaeogeogr. Palaeoclimatol. Palaeo- ecol*., 62, 237–270.

De Vicente, G., González-Casado, J.M., Muñoz-Martín, A., Giner, J. and Rodríguez-Pascua, M.A. (1996) Structure and Tertiary evolution of the Madrid Basin. In: *Tertiary Basins of Spain. The Stratigraphic Record of Crustal Kinematics* (Eds P.F. Friend and C.J. Dabrio), pp. 263–267. Cambridge University Press, Cambridge.

Esteban, M. (1991) Palaeokarst: Practical applications. In: *Palaeokarsts and Palaeokarstic Reservoirs* (Ed. V.P. Wright), pp. 89–119. PRIS Occasional Publication Series no. 2. University of Reading, Reading.

Esteban, M. and Klappa, C.F. (1983) Subaerial exposure environment. In: *Carbonate Depositional Environments* (Eds P.A. Scholle, D.G. Bebout and C.H. Moore), *Am. Assoc. Petrol. Geol. Mem*., 33, 1–54.

Ford, D.C. (1988) Characteristics of dissolutional cave systems in carbonate rocks. In: *Paleokarst* (Eds N.P. James and P.W. Choquette), pp. 25–57. Springer-Verlag, New York.

Ford, D.C. and Williams, P.W. (1989) *Karst Geomorphology and Hydrology*. Unwin-Hyman, London, 601 pp.

Forti, P. (1993) Karst evolution and water circulation in gypsum formations. In: *Proceedings International Symposium on Water Research in Karst with Special Emphasis in Arid and Semi-Arid Zones, Shiraz, Iran*, pp. 791–801.

Friedman, G.M. (1997) Dissolution-collapse breccias and paleokarst resulting from dissolution of evaporite rocks, especially sulfates. *Carbonates Evaporites*, 12, 53–63.

Gunatilaka, A. (1990) Anhydrite diagenesis in a vegetated sabkha, Al-Khiram, Kuwait, Arabian Gulf. *Sed. Geol*., 69, 95–116.

Gunatilaka, A., Saleh, A. and Al-Temeemi, A. (1980) Plant-controlled supratidal anhydrite from Al-Khiran, Kuwait. *Nature*, 288, 257–260.

Gutiérrez, F. (1996) Gypsum karstification induced subsidence: effects on alluvial systems and derived geohazards (Calatayud Graben, Iberian Range, Spain). *Geomorphology*, 16, 277–293.

Halfar, J., Riegel, W. and Walther, H. (1998) Facies architecture and sedimentology of a meandering fluvial system: a Palaeogene example from the Weisselster Basin, Germany. *Sedimentology*, 45, 1–17.

Hammer, U.T. (1986) *Saline Lake Ecosystems of the World*. Junk, Dordrecht, 616 pp.

Hardie, L.A., Smoot, J.P. and Eugster, H.P. (1978) Saline lakes and their deposits: a sedimentological approach. In: *Modern and Ancient Lake Sediments* (Eds A. Matter and M.E. Tucker), *Spec. Publ. Int. Assoc. Sedimentol*., 2, 7–41.

Hill, C.A. and Forti, P. (1977) *Cave Minerals of the World*. National Speleological Society, Huntsville, 258 pp.

James, N.P. and Choquette, P.W. (eds) (1988) *Paleokarst*. Springer Verlag, New York, 416 pp.

Jennings, J.N. (1971) *Karst*. The MIT Press, Cambridge, MA, 252 pp.

Jennings, J.N. (1985) *Karst Geomorphology*. Basil Blackwell, Oxford, 293 pp.

Johnson, K.S. and Neal, J.T. (co-ords) (1997) Symposium on evaporite karst: origins, processes, landforms, examples, and impacts. *Carbonates Evaporites*, 12, 1.

Klappa, C.F. (1980) Rhizoliths in terrestrial carbonates: classification, recognition, genesis and significance. *Sedimentology*, 27, 613–629.

Klimchouk, A. (1996a) The typology of gypsum karst according to its geological and geomorphological evolution. *Int. J. Speleol*., 25, 49–59.

Klimchouk, A. (1996b) Speleogenesis in gypsum. *Int. J. Speleol*., 25, 61–82.

Klimchouk, A., Lowe, D., Cooper, A. and Sauro, U. (eds) (1996a) Gypsum karst of the world. *Int. J. Speleol*., 25, 307 pp.

Klimchouk, A., Cucchi, F., Calaforra, J.M., Aksem, S., Finocchiaro, F. and Forti, P. (1996b) Dissolution of gypsum from field observations. *Int. J. Speleol.*, 25, 37–48.

Last, W.M. (1993) Salt dissolution features in saline lakes of the northern Great Plains, western Canada. *Geomorphology*, 8, 321–334.

Loucks, R.G. (1999) Paleocave carbonate reservoirs: origins, burial-depth modifications, spatial complexity, and reservoir implications. *AAPG Bull.*, 83, 1795–1834.

Macaluso, T. and Sauro, U. (1996) Weathering crust and karren on exposed gypsum surfaces. *Int. J. Speleol.*, 25, 115–126.

Ordóñez, S., Calvo, J.P., García del Cura, M.A., Alonso Zarza, A.M. and Hoyos, M. (1991) Sedimentology of sodium sulphate deposits and special clays from the Tertiary Madrid Basin (Spain). In: *Lacustrine Facies Analysis* (Eds P. Anadón, L. Cabrera and K. Kelts), *Spec. Publ. Int. Assoc. Sedimentol.*, 13, 39–55.

Peerman, S. and Belski, D. (1991) Gypscap, another New Mexico caving project. *NSS News*, February, 57–63.

Pierre, C. and Rouchy, J.M. (1988) Carbonate replacements after sulphate evaporites in the Middle Miocene of Egypt. *Sed. Petrol.*, 58, 446–456.

Pomar, L., Ginés, A. and Fortanau, R. (1976) Las cristalizaciones freáticas. *Endines*, 3, 3–25.

Powers, D.W. and Hassinger, B.W. (1985) Synsedimentary dissolution pits in halite of the Permian Salado Formation, southeastern New Mexico. *Sed. Petrol.*, 55, 769–773.

Rodríguez-Aranda, J.P. (1995) *Sedimentología de los Sistemas de Llanura Lutítica-lago Salino del Mioceno en la Zona Oriental de la Cuenca de Madrid (Tarancón-Aunón)*. PhD Thesis, Universidad Complutense, Madrid, 474 pp.

Rodríguez-Aranda, J.P. and Calvo, J.P. (1997) Desarrollo de paleokarstificación en facies yesíferas del Mioceno de la Cuenca de Madrid. Implicaciones en el análisis evolutivo de sucesiones lacustres evaporíticas. *Bol. Geol. Min.*, 108, 377–392.

Rodríguez-Aranda, J.P. and Calvo, J.P. (1998) Trace fossils and rhizoliths as a tool for sedimentological and palaeoenvironmental analysis of ancient continental evaporite successions. *Palaeogeogr. Palaeoclimatol. Palaeoecol.*, 140, 383–399.

Rodríguez-Aranda, J.P., Calvo, J.P. and Sanz-Montero, M.E. (1996) Paleokarstificación en facies yesíferas e implicaciones sedimentarias. Ejemplos del Mioceno de la Cuenca de Madrid. *Geogaceta*, 20, 327–330.

Sanz, M.E., Rodríguez-Aranda, J.P., Calvo, J.P. and Ordóñez, S. (1994) Tertiary detrital gypsum in the Madrid Basin, Spain: criteria for interpreting detrital gypsum in continental evaporitic sequences. In: *Sedimentology and Geochemistry of Modern and Ancient Saline Lakes* (Eds R.W. Renaut and W.M. Last), *SEPM Spec. Publ.*, 50, 217–228.

Sanz-Montero, M.E. (1996) *Sedimentología de las Formaciones Neógenas del sur de la Cuenca de Madrid, con Énfasis en los Procesos Kársticos y Edáficos Asociados a las Rupturas Sedimentarias del Plioceno*. PhD Thesis, University Complutense, Madrid, 245 pp.

Sanz-Rubio, E., Sánchez-Moral, S., Cañaveras, J.C., Calvo, J.P. and Rouchy, J.M. (2001) Calcitization of Mg-Ca carbonate and Ca sulphate deposits in a continental Tertiary basin (Calatayud Basin, NE Spain). *Sed. Geol.*, 140, 123–142.

Sauro, U. (1996) Geomorphological aspects of gypsum karst areas with special emphasis on exposed karst. *Int. J. Speleol.*, 25, 105–114.

Schreiber, C.B. and El Tabakh, M. (2000) Deposition and early alteration of evaporites. *Sedimentology*, 47 (Suppl. 1), 215–238.

Smart, P.L. and Whitaker, F.F. (1991) Karst processes, hydrology and porosity evolution. In: *Palaeokarsts and Palaeokarstic Reservoirs* (Ed. V.P. Wright), pp. 1–55. PRIS Occasional Publication Series no. 2. University of Reading, Reading.

Thraikill, J. (1968) Chemical and hydrologic factors in the excavation of limestone caves. *Bull. Geol. Soc. Am.*, 87, 19–46.

Vanstone, S.D. (1998) Late Dianantian palaeokarst of England and Wales: implications for exposure surface development. *Sedimentology*, 45, 19–37.

Warren, J. (1999) *Evaporites. Their Evolution and Economics*. Blackwell Science, Oxford, 438 pp.

Warren, J.K., Havholm, K.G., Rosen, M.R. and Parsley, M.J. (1990) Evolution of gypsum karst in the Kirschberg Evaporite Member near Fredericksburg, Texas. *J. Sed. Petrol.*, 60, 721–734.

Wright, V.P. (1982) The recognition and interpretation of paleokarsts: two examples from the Lower Carboniferous of South Wales. *J. Sed. Petrol.*, 52, 83–94.

Wright, V.P. (1991) Palaeokarst: types, recognition, controls and associations. In: *Palaeokarsts and Palaeokarstic Reser- voirs* (Ed. V.P. Wright), pp. 56–88. PRIS Occasional Publi- cation Series no. 2. University of Reading, Reading.

Yaoru, L. and Cooper, A.H. (1996) Gypsum karst in China. *Int. J. Speleol.*, 25, 297–307.